Synthesis of $Ag_{core}Au_{shell}$ Bimetallic Nanoparticles for Immunoassay Based on Surface-Enhanced Raman Spectroscopy

Yan Cui,[†] Bin Ren,*[,‡] Jian-Lin Yao,[†] Ren-Ao Gu,*[,†] and Zhong-Qun Tian[‡]

Department of Chemistry, Suzhou University, Suzhou 215006, China, and State Key Laboratory for Physical Chemistry of Solid Surfaces and College of Chemistry and Chemical Engineering, Xiamen University, Xiamen 361005, China

Received: October 28, 2005; In Final Form: December 28, 2005

Layered core−shell bimetallic silver−gold nanoparticles were prepared by coating Au layers over Ag seeds by a seed-growth method. The composition of $Ag_{100-x}Au_x$ particles can vary from $x = 0$ to 30. TEM and SEM images clearly show that the bimetallic nanoparticles are of core−shell structure with some pinholes on the surface. Strong surface-enhanced Raman (SER) signals of thiophenol and *p*-aminothiophenol have been obtained with these colloids. It was found that the SERS activity of aggregated colloids critically depends on the molar ratio of Ag to Au. With the increase of the Au molar fraction, the SERS activity enhances first and then weakens, with the maximal intensity being 10 times stronger than that of Ag colloids. The $Ag_{core}Au_{shell}$ nanoparticles were then labeled with monoclonal antibodies and SERS probes and used for immunoassay analysis. In the proposed system, antibodies immobilized on a solid substrate can interact with the corresponding antigens to form a composite substrate, which can capture reporter-labeled $Ag_{core}Au_{shell}$ nanoparticles modified with the same antibodies. The immunoreaction between the antibodies and antigens was demonstrated by the detection of characteristic Raman bands of the probe molecules. $Ag_{core}Au_{shell}$ bimetallic nanoparticles, as a new SERS active and biocompatible substrate, will be expected to improve the detection sensitivity of immunoassay.

Introduction

The detection of biomolecules by optical means is of particular interest in areas such as pharmaceuticals and biowarfare agent detection.[1] Recently, Raman spectroscopy has been extensively employed to investigate biological molecules and materials. One of the main advantages of Raman spectroscopy is that it can provide rich structural information as well as quantitative and qualitative information about molecules. This is of particular interest for bio-applications, where specificity of detection is important. Other than in the case of IR and NMR spectroscopy, Raman measurements will not be interfered by the presence of water commonly existing in all biological samples.[2] Moreover, unlike fluorescence processes, which usually produce relatively broad bands, Raman process is directly related to the vibration mode of molecules, which yields very narrow and characteristic Raman bands allowing one to distinguish even very similar molecules.[3] However, conventional Raman spectroscopy usually lacks sufficient sensitivity for use as a readout method for the low concentration bioanalysis.

Surface-enhanced Raman spectroscopy, on the other hand, has attracted much greater attention for use as a bioanalytical method since the report of single-molecule sensitivity.[4,5] It is capable of detecting picomole to femtomole amounts of species on several types of roughened metal surfaces.[6] It has been applied to areas such as chemical sensing,[7,8] medical diagnostics,[9,10] and the study of living cells[11] and bacteria.[12] Recently, there is an increasing number of reports on the use of SERS in immunoassay.

Immunoassay is a common and useful means of biochemical analysis.[13] The strong, specific binding of an antibody to its antigen has been widely exploited in biochemical studies, clinical diagnostics, sensor design, and environmental monitoring. In past years, many different approaches such as scintillation counting,[14] fluorescence,[15] chemiluminescence,[16] electrochemical detection,[17] enzymatic,[18] and surface plasmon resonance (SPR)[19] have been developed for a direct measurement of antigen−antibody binding. The use of SERS for enzyme immunoassay dates back to the end of the 1980s, when Cotton et al. employed the SERRS effect to detect human thyroid simulating hormone (TSH) antigen.[20] Since then, there have been continuous reports on SERS as an immunoassay method.[21−25]

Au and Ag colloids are metallic systems largely employed in SERS.[26,27] In comparison with Ag, Au colloidal particles have many advantages, including easy preparation, high homogeneity,[28] and biocompatibility with antibody or antigen[29] and DNA or RNA.[30] For these reasons, Au colloidal particles have been applied extensively in gene analysis and antibody or antigen detection.[23−24,31] However, the Au surface shows a lower enhancement in the visible light region in comparison with that of Ag.[32] Therefore, there have been many attempts to obtain core−shell particles by depositing Ag on preformed Au particles to achieve a higher signal than that from bare Au nanoparticles.[33−35] $Au_{core}Ag_{shell}$ nanoparticles have been applied in the gene analysis and antibody or antigen detection in vitro.[36] Ag staining enhancement method has also been applied for a similar purpose.[37,38] However, it should be noted that Ag is not considered biocompatible.[39] If the reverse structure, that is, $Ag_{core}Au_{shell}$ nanoparticles, can be used for immunoassay, then,

* To whom correspondence should be addressed. R. A. Gu: telephone, +86-512-65882892; fax, +86-512-65231918; e-mail, ragu@suda.edu.cn. B. Ren: telephone, +86-592-2181906; e-mail, bren@xmu.edu.cn.

[†] Suzhou University.

[‡] Xiamen University.

10.1021/jp056203x CCC: $33.50
Published on Web 02/04/2006

SCHEME 1. Schematic Illustration of the Process of a Self-Assembled Sandwich Structure Immobilized on a Substrate Using Reporter-Labeled Immuno-$Ag_{core}Au_{shell}$ Bimetallic Nanoparticles

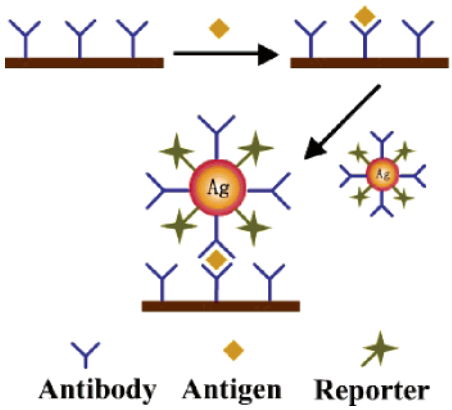

on one hand, they are biocompatible and, on the other hand, the underneath Ag core may provide extra enhancement to the Au surface. The research on such a structure is comparatively less.[40,41] As far as we know, there is to date no report on using $Ag_{core}Au_{shell}$ nanoparticles for immunoassay.

In the present paper, layered core−shell $Ag_{core}Au_{shell}$ bimetallic nanoparticles were prepared by depositing Au over Ag seeds using the seed-growth method. Interestingly, we found that the pinholes appearing on the surfaces of $Ag_{core}Au_{shell}$ bimetallic nanoparticles result in a large SERS enhancement of the adsorbed thiophenol (TP) and *p*-aminothiophenol (PATP). We further used the $Ag_{core}Au_{shell}$ bimetallic nanoparticles as the SERS enhancing substrate to detect the interaction between the antibody and antigen in immunoassay combined with the molecule labeling method. For clarity, we depict in Scheme 1 the method used in the present paper, which is similar to that proposed by Ni et al.:[23] the antibodies are immobilized on a solid substrate first, which will then interact with the corresponding antigens in the sample to form a composite substrate. Finally, the substrate can capture reporter-labeled $Ag_{core}Au_{shell}$ nanoparticles modified with same antibodies, forming a sandwich-type complex "capture antibody substrate/antigen/reporter-labeled immuno-$Ag_{core}Au_{shell}$ bimetallic nanoparticles". The final complex was then detected by Raman spectroscopy. The binding specificity was successfully demonstrated by the detection of characteristic Raman bands of the probe molecules.

Experimental Section

Reagents and Immunoreaction Buffers. Goat anti mouse IgG, bovine serum albumin (BSA), and Tween 80 were purchased from Sino-Amercian Biotechnology Co. Mouse IgG and human IgG were acquired from Sigma. *p*-Aminothiophenol (PATP) was obtained from Lancaster. Thiophenol (TP), hydroxylamine hydrochloride ($NH_2OH{\cdot}HCl$), trisodium citrate, and tris(hydroxymethyl)aminomethane (Tris) were purchased from Shanghai Reagents Co. (Shanghai, China). Chloroauric acid ($HAuCl_4{\cdot}4H_2O$) and silver nitrate ($AgNO_3$) were obtained from Sinopharm Chemical Reagent Co., Ltd. Ultrapure water with a conductivity of 18MΩ cm^{-1} was used in all experiments.

The following buffer solutions were used: borate buffer (BB, 2 mM, pH = 9), PBS buffer (KH_2PO_4/K_2HPO_4, 150 mM NaCl, pH = 7.6), TBS buffer (10 mM Tris, 150 mM NaCl, pH = 7−8), and TBS/0.1% Tween buffer (10 mM Tris, 150 mM NaCl, 0.1% Tween, pH = 7−8).

Preparation of Raman Reporter-Labeled Immuno-$Ag_{core}Au_{shell}$ Bimetallic Nanoparticles. $Ag_{core}Au_{shell}$ bimetallic nanoparticles were prepared by deposition of Au on the preformed ∼50 nm Ag nanoparticles. The initial Ag colloid was prepared according to Lee and Meisel's method:[42] In a typical process, 250 mL of a 5.29×10^{-4} M $AgNO_3$ aqueous solution was heated to boiling with vigorous stirring, to which 5 mL of a 1% trisodium citrate solution was added. The mixture was then kept boiling for 1 h. Afterward, the solution was allowed to cool to room temperature with continuous stirring. $Ag_{core}Au_{shell}$ bimetallic nanoparticles with varying molar fractions of Au were prepared following the literature procedure with a slight modification.[43] Briefly, to 12.5 mL of Ag colloid diluted with 10 mL of ultrapure water, *x* mL of 6.25×10^{-3} M $NH_2OH{\cdot}HCl$ and *x* mL of 4.65×10^{-4} M $HAuCl_4$ were added dropwise (ca. 2 mL/min) by two separate pipets upon vigorous stirring. The stirring was continued for 45 min.

Next, 1 μL of 1 mM probe molecule (TP or PATP) in ethanol was added to 1.0 mL of $Ag_{core}Au_{shell}$ bimetallic nanoparticles, and the resultant mixture was allowed to react for 1 h. The amount of thiol, based on an estimation of the surface area of nanoparticles, was chosen to coat only a portion of the nanoparticles surface. The reporter-labeled nanoparticles were then separated from the solution by centrifugation at 6000*g* for 20 min and resuspended with 1.0 mL of borate buffer. Next, 20 μL of 1.0 mg/mL goat anti mouse IgG was added to 1.0 mL of TP-labeled $Ag_{core}Au_{shell}$ bimetallic nanoparticles. This amount of antibody is ∼50% more than the minimum amount for coating the unmodified portion of the nanoparticles surface. After incubation at room temperature for 1 h, the TP-labeled immuno-$Ag_{core}Au_{shell}$ bimetallic nanoparticles were purified by centrifugation and resuspended with 1.0 mL of the borate buffer. To make sure that no bare sites were left, 10 μL of BSA (2% m/m) was added to the above TP-labeled immuno-$Ag_{core}Au_{shell}$ bimetallic nanoparticles. The mixture was incubated for 60 min at room temperature, and then centrifugated and resuspended in 1.0 mL of borate buffer.

Preparation of Capture Antibody Substrates. The substrates were microscopic glass slides coated with multiple layers of materials as described below and were donated by Full Moon BioSystems. The slide surface was first coated with a buffer layer of Ni−Cr using a vacuum deposition process and then coated with a thin layer of silver. After being activated, the surface was covered with a polymer layer, which contains specifically designed functional groups that can bind to the −COOH groups of antibodies. This particular binding arrangement allows antibodies to be erected on the surface without compromising their biological activities.

Next, 100 μL of goat anti mouse IgG (100 μg/mL in 0.1 M borate buffer, pH = 9) was dropped onto the 1-cm^2 substrate. After being placed in a chamber with a relative humidity of 65−75% for over 12 h, the substrates were allowed to dry at room temperature for 30 min. The substrates were then incubated in 5% BSA for 1 h to block active sites between antibodies, rinsed with water, and dried under nitrogen.

Immunoassay Protocol. The immunoassays were conducted following the typical procedure for a sandwich-type assay. Goat IgG and human IgG were used as the test antigen. In each case, 100 μL of IgG solution (1μg/mL) was diluted in 1 mL of 50 mM PBS buffer in a tube, and then the capture antibody-coated substrate was immersed in the above solution. After the tube had been gently shaken at room temperature for about 2−4 h on a shaker, the substrates were taken out and washed three times with TBS/0.1% Tween at room temperature and then washed two times with TBS. After being rinsed with copious amounts of water, the substrates were placed in a tube containing

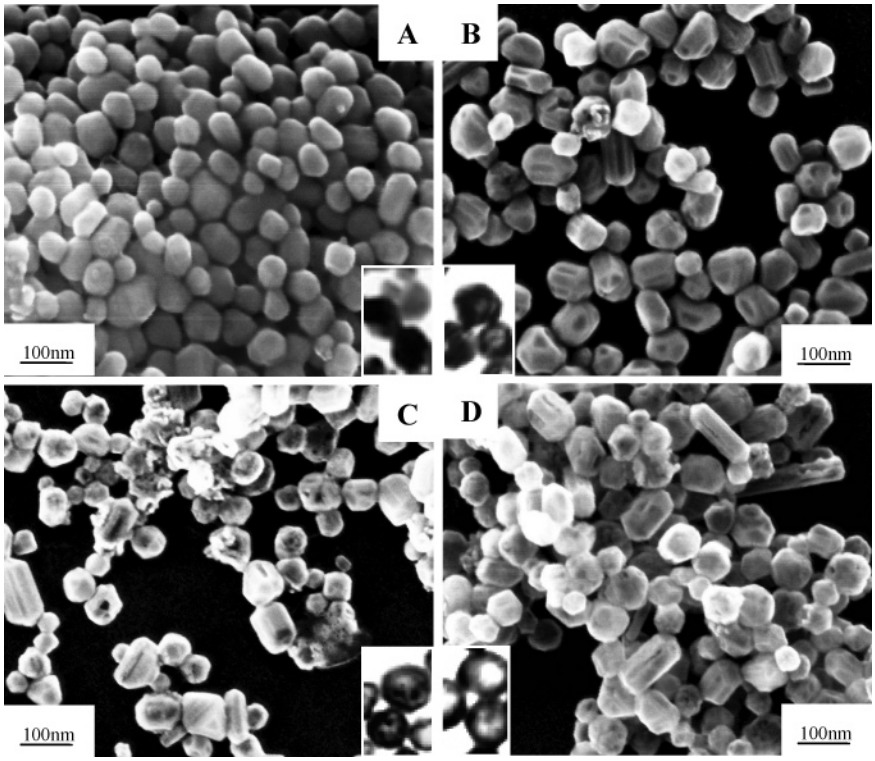

Figure 1. SEM images of silver nanoparticles (A) and $Ag_{core}Au_{shell}$ with different molar ratios: $Ag_{97}Au_3$ (B), $Ag_{88}Au_{12}$ (C), and $Ag_{70}Au_{30}$ (D). The insets are the corresponding TEM images.

reporter-labeled immuno-$Ag_{core}Au_{shell}$ bimetallic nanoparticles. The tube was gently shaken at room temperature for 2 h, and then all of the samples were rinsed with TBS/0.1% Tween, TBS, and deionized water successively and then dried under nitrogen.

Instrumentation. Raman spectra were obtained using a confocal microprobe Raman system (LabRam I, Dilor).[44] It is a single spectrograph instrument equipped with a holographic notch filter and a CCD detector. The sizes of the slit and pinhole were 200 and 800 μm, respectively. A long working distance 50× objective was used to collect the Raman scattering signal. The excitation wavelength was 632.8 nm from a He−Ne laser. Scanning electron microscopy (SEM) was taken with a field-emission microscope (Leo1530) operated at an accelerating voltage of 20 kV. Transmission electron microscopy (TEM) was performed with a JEM-200 CX microscope operated at 100 kV.

Results and Discussion

Morphological and Structural Changes of Bimetallic Nanoparticles. SEM images of Ag nanoparticles and Ag_{core}-Au_{shell} bimetallic nanoparticles prepared by adding various amounts of $HAuCl_4$ to the same amount of parent Ag seeds are shown in Figure 1, and the insets are the corresponding TEM images. Figure 1A gives an SEM image of the Ag seeds with a mean diameter of ~60 ± 10 nm. Because the standard reduction potential of the $AuCl_4^-$/Au pair (0.99 V vs standard hydrogen electrode, SHE) is higher than that of the Ag^+/Ag pair (0.80 V vs SHE), silver will be oxidized into Ag^+ when silver nanoparticles and $HAuCl_4$ are mixed in an aqueous medium: $3Ag\ (s) + AuCl_4^-\ (aq) \rightarrow Au\ (s) + 3Ag^+\ (aq) + 4Cl^-\ (aq)$.[45−47] After Ag nanoparticles had reacted with a very small amount (i.e., 0.5 mL) of $HAuCl_4$ and $NH_2OH{\cdot}HCl$ solution, some striae appeared on the surface of Ag seeds. As shown in Figure 1B, the appearance of striae at a specific spot on each Ag nanoparticle indicates that the replacement reaction was initiated locally rather than over the entire surface. The newly formed surfaces containing striae should act as the most active sites for further replacement reaction. As more $HAuCl_4$ and $NH_2OH{\cdot}HCl$ solution (i.e., 2.0 mL) reacted with Ag nanoparticles, some of the striae turned into small pinholes (Figure 1C). Meanwhile, $HAuCl_4$ was reduced by $NH_2OH{\cdot}HCl$, forming a Au layer on the Ag nanoparticle surfaces. From the TEM image in Figure 1C, the color of the center of most particles was lighter than its edge, indicating the formation of a core−shell nanostructure.[45] The Au atoms resulting from both the galvanic replacement reaction and the reduction reaction tend to be epitaxially deposited on the surfaces of Ag seeds for two reasons: the first one is their close match in the crystal structure (both silver and gold have a face-centered cubic lattice) and lattice parameters (4.0786 and 4.0862 Å for gold and silver, respectively),[48] and the second reason is that $NH_2OH{\cdot}HCl$, the reducing agent used in this study, is known to be very efficient for deposition of a second metal layer over nuclei (parent colloid).[49,50] From the figure, we can also see that no new particles nucleation occurs in solution in this step. The Au shell on each individual Ag nanoparticle prevents the underneath Ag surface from reacting with $HAuCl_4$. As a result, when the volume of $HAuCl_4$ and $NH_2OH{\cdot}HCl$ solution was further increased (i.e., 4.0 mL), the $AuCl_4^-$ ions were mainly reduced by $NH_2OH{\cdot}HCl$ to Au atoms that coat on the Ag nanoparticles to form a complete Au shell. From the SEM in Figure 1D, there is almost no pinhole on the surface and the mean diameters of the whole nanoparticles are larger than the Ag seeds because of the formation of the Au shell. The TEM image of prepared $Ag_{70}Au_{30}$ in the inset of Figure 1D displays a clear core−shell contrast.

SERS Activity of $Ag_{core}Au_{shell}$ Bimetallic Nanoparticles. $Ag_{core}Au_{shell}$ nanoparticles are expected to be SERS-active because both the core and the shell layers are well-known SERS-active materials. In our experiment, TP and PATP were used as the probing molecules, because of their well-established

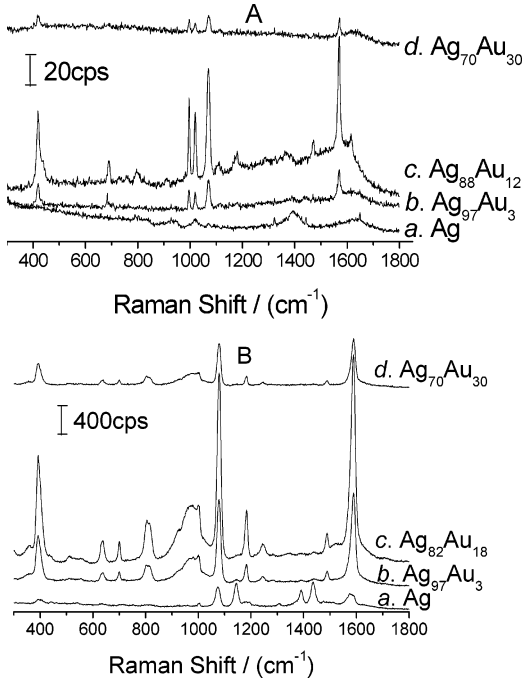

Figure 2. SERS spectra of TP (A) and PATP (B) on different colloids: (a) Ag, (b) $Ag_{97}Au_3$, (c) $Ag_{82}Au_{18}$, and (d) $Ag_{70}Au_{30}$.

Raman spectral data and large Raman scattering cross section.[51−53] Figure 2 displays the SER spectra for 1×10^{-6} M TP and PATP adsorbed on the Ag and $Ag_{core}Au_{shell}$ bimetallic nanoparticles at an excitation wavelength of 632.8 nm. In the literature, it was found that the SERS activity of the $Ag_{core}Au_{shell}$ colloids sits between the activities of Ag and Au.[40] Here, we found that the SERS signal intensity is dependent on the Ag:Au ratio of these core−shell colloids: with the increase of the Au fraction, the SERS activity enhances first and then weakens, with the maximal intensity being 10 times stronger than that of Ag colloids. An issue that needs to be further addressed is the presence of pinholes on core−shell nanoparticles. It is important to determine whether the SERS intensity comes from the Ag core or not. Ag has been considered to be more SERS-active than Au.[32] However, in the present study, the absolute Raman intensity from Ag nanoparticles is less than that from Ag_{core}-Au_{shell} nanoparticles. Therefore, the interference of the Ag core can be neglected. The DDA calculation of Hao et al. indicates that the pinholes provide hot spots for electromagnetic field enhancement and and the $|E|^2$ can be 3−4 times larger or even 10 times larger than that of the seamless nanoshells.[54] This result means that the molecules in the pinholes will show about 10−100 times higher SERS enhancements than those on perfect shells. The significance of this enhancement would depend on the pinhole density. If more than 10% of the surface area is covered by pinholes, then the contributions of pinholes to the SERS measurements could exceed the rest of the surface. As shown in Figure 1, with the increase of Au molar ratio, some pinholes appeared on the surface of Ag seeds and then were coated with a Au shell. The number of pinholes reaches the maximum at $Ag_{88}Au_{12}$. The essential feature is that when there are some pinholes on the surface, the SERS signal is enhanced, and when the surface is fully coated with a Au shell, the signal is weakened. We also found that the signal intensity of PATP is significantly higher than that of TP, which cannot be understood solely by the difference in the Raman scattering cross sections of the two molecules, because the excitation is out of the resonance region and the two molecules have similar structures. Furthermore, there is not much difference in the Raman feature (relative intensity and frequency) when TP is adsorbed on nanoparticles with different molar fractions of Au; however, a significant difference in the SER spectra was observed for PATP. After considering all of these effects, the difference in the relative intensities for the two molecules might be explained by the participation of the CT mechanism.[51]

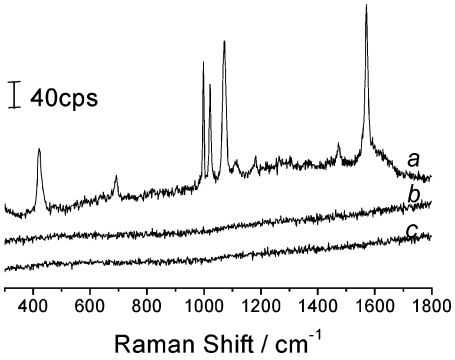

Figure 3. SERS spectra of (a) the "sandwich" construction labeled by TP, (b) the "sandwich" construction without antigen, and (c) the "sandwich" construction with irrelevant antigen.

Immunoassay Using TP as the Probing Molecule. Before going into the details of the immunoassay experiment, it is necessary to emphasize the two important characters of the interaction between the antibody and antigen: first, antibody molecules interact highly specifically with their corresponding antigens; for example, goat anti mouse IgG can specifically bind to mouse IgG but will not bind to human IgG; second, antigens are often multivalent in their interactions with antibodies.

To test the feasibility of combining the SERS method and reporter-labeled immuno-$Ag_{core}Au_{shell}$ bimetallic nanoparticles to detect the presence of specific antigenic species in an aqueous sample, we carried out the immunoassay experiments as described in detail in the Experimental Section. These experiments used $Ag_{core}Au_{shell}$ nanoparticles that had been labeled with TP molecules as the Raman reporter and the goat anti mouse IgG for immunorecognition. In a typical process, the substrate coated with goat anti mouse IgG was exposed to a solution containing antigen (mouse IgG, 100 μg/mL); see the second step in Scheme 1. After incubation for 4 h, the sample was developed in the TP-labeled immuno-$Ag_{core}Au_{shell}$ bimetallic nanoparticles suspension for 2 h. By this process, the mouse IgG was first bound to the corresponding goat anti mouse IgG previously immobilized on the substrate, and then it will capture the same antibody that has been immobilized on the labeled $Ag_{core}Au_{shell}$ bimetallic nanoparticles; see the third step in Scheme 1. Thus, a sandwiched structure "capture antibody substrate/antigen/Raman reporter-labeled immuno-$Ag_{core}Au_{shell}$ bimetallic nanoparticles" will be constructed. The SERS signal obtained from such substrate is presented in Figure 3a. The strong SERS signals at 420, 690, 998, 1072, and 1571 cm^{-1} are from TP, and the result is consistent with the binding specificity in a sandwich-type assay for mouse IgG. The specificity of the labeled immuno-$Ag_{core}Au_{shell}$ nanoparticles was also tested by two control experiments using human IgG (100 μg/mL) and PBS buffer free of any antigen (Figure 3b,c). Mouse IgG can be captured by the substrate but not the human IgG, and if there is no antigen, the sandwiched structure will also not be constructed. The bands evident in the latter two spectra for either human IgG or PBS buffer are barely above the background, which is in agreement with the lack of specificity as expected. The results of these experiments indicate that the $Ag_{core}Au_{shell}$ bimetallic nanoparticles could be used as a good SERS substrate for the immunoassay analysis.

Conclusions

We have presented here a seed growth method to prepare $Ag_{core}Au_{shell}$ bimetallic nanoparticles. With the increase of the Au molar fraction, some pinholes appeared on the surface, which was then coated with a complete Au shell. Correspondingly, the SERS intensity of probe molecules such as TP and PATP adsorbed on the bimetallic nanoparticles enhanced first and then weakened, with the maximal intensity being 10 times higher than that on Ag. This interesting result could be attributed to the presence of some pinholes that act as hot spots for the electromagnetic field enhancement. The immunoreactions between the labeled immuno-$Ag_{core}Au_{shell}$ bimetallic nanoparticles and the corresponding antigens captured by goat anti mouse IgG on the substrates have been investigated by SERS. This primary study demonstrates that the $Ag_{core}Au_{shell}$ bimetallic nanoparticles labeled by the monoclonal antibodies and SERS probes could be used for immunoassay analysis.

Acknowledgment. We gratefully acknowledge the support from the Natural Science Foundation of China (NSFC) (20373046, 20573076, 90206039), the MOE of China (20040384010), the NSF of Jiangsu Province (BK2005032), and the State Key Laboratory for Physical Chemistry of Solid Surfaces of Xiamen University. All of the experiments were carried out at Xiamen University. We also thank Full Moon BioSystems Inc. (www.fullmoonbiosystems.com, Sunnyvale, CA) for the kind donation of the substrates for our experiment.

References and Notes

(1) Drachev, V. P.; Thoreson, M. D.; Nashine, V.; Khaliullin, E. N.; Ben-Amotz, D.; Davisson, V. J.; Shalaev, V. M. *J. Raman Spectrosc.* **2005**, *36*, 648.

(2) Gessner, R.; Rosch, P.; Petry, R.; Schmitt, M.; Strehle, M. A.; Kiefer, W.; Popp, J. *Analyst* **2004**, *129*, 1193.

(3) Kneipp, K.; Kneipp, H.; Itzkan, I.; Dasari, R. R.; Feld, M. S. *Chem. Rev.* **1999**, *99*, 2957.

(4) Nie, S.; Emory, S. R. *Science* **1997**, *275*, 1102.

(5) Kneipp, K.; Wang, Y.; Kneipp, H.; Perelman, L. T.; Itzkan, L.; Dasari, R. R.; Feld, M. S. *Phys. Rev. Lett.* **1997**, *78*, 1667.

(6) Garrell, R. L. *Anal. Chem.* **1989**, *61*, 401A.

(7) Alak, A. L.; Vo-Dinh, T. *Anal. Chem.* **1987**, *59*, 2149.

(8) Bello, J. M.; Stokes, D. L.; Vo-Dinh, T. *Anal. Chem.* **1989**, *61*, 1779.

(9) Volkan, M.; Stokes, D. L.; Tuan, V. D. *Appl. Spectrosc.* **2000**, *54*, 1842.

(10) Allain, L. R.; Vo-Dinh, T. *Anal. Chim. Acta* **2002**, *469*, 149.

(11) Kneipp, K.; Haka, A. S.; Kneipp, H.; Badizadegan, K.; Yoshizawa, N.; Boone, C.; Shafer-Peltier, K. E.; Motz, J. T.; Dasari, R. R.; Feld, M. S. *Appl. Spectrosc.* **2002**, *56*, 150.

(12) Premasiri, W. R.; Moir, D. T.; Klempner, M. S.; Krieger, N.; Jones, G.; Ziegler, L. D. *J. Phys. Chem. B* **2005**, *109*, 312.

(13) Kanda, V.; Kariuki, J. K.; Harrison, D. J.; McDermott, M. T. *Anal. Chem.* **2004**, *76*, 7257.

(14) Gutcho, S.; Mansbach, L. *Clin. Chem.* **1977**, *23*, 1609.

(15) Bruchez, M.; Moronne, M.; Gin, P.; Weiss, S.; Alivisatos, A. P. *Science* **1998**, *281*, 2013.

(16) Yakovleva, J.; Davidsson, R.; Lobanova, A.; Bengtsson, M.; Eremin, S.; Laurell, T.; Emneus, J. *Anal. Chem.* **2002**, *74*, 2994.

(17) Duan, C.; Meyerhoff, M. E. *Anal. Chem.* **1994**, *66*, 1369.

(18) Gosling, J. P. *Clin. Chem.* **1990**, *36*, 1408.

(19) Oh, B. K.; Kim, Y. K.; Lee, W.; Bae, Y. M.; Lee, W. H.; Choi, J. W. *Biosens. Bioelectron.* **2003**, *18*, 605.

(20) Rohr, T. E.; Cotton, T.; Fan, N.; Tarcha, P. J. *Anal. Biochem.* **1989**, *182*, 388.

(21) Dou, X.; Takama, T.; Yamaguchi, Y.; Yamamoto, H. *Anal. Chem.* **1997**, *69*, 1492.

(22) Dou, X.; Yamaguchi, Y.; Yamamoto, H.; Doi, S.; Ozaki, Y. *J. Raman Spectrosc.* **1998**, *29*, 739.

(23) Ni, J.; Lipert, R. J.; Dawson, G. B.; Porter, M. D. *Anal. Chem.* **1999**, *71*, 4903.

(24) Grubisha, D. S.; Lipert, R. J.; Park, H.-Y.; Driskell, J.; Porter, M. D. *Anal. Chem.* **2003**, *75*, 5936.

(25) Mulvaney, S. P.; Musick, M. D.; Keating, C. D.; Natan, M. J. *Langmuir* **2003**, *19*, 4784.

(26) Sanchez-Cortes, S.; Garcia-Ramos, J. V.; Morcillo, G. *J. Colloid Interface Sci.* **1994**, *167*, 428.

(27) Blatchford, C. G.; Campbell, J. R.; Creighton, J. A. *Surf. Sci.* **1982**, *120*, 435.

(28) Sutherland, W. S.; Winefordner, J. D. *J. Colloid Interface Sci.* **1992**, *148*, 129.

(29) Mann, S.; Shenton, W.; Li, M.; Connolly, S.; Fitzmaurice, D. *Adv. Mater.* **2000**, *12*, 147.

(30) Mirkin, C. A.; Letsinger, R. L.; Mucic, R. C.; Storhoff, J. J. *Nature* **1996**, *382*, 607.

(31) Ma, Z. F.; Sui, S. F. *Angew. Chem., Int. Ed.* **2002**, *41*, 2176.

(32) Laserna, J. J. *Anal. Chim. Acta* **1993**, *283*, 607.

(33) Freeman, R. G.; Hommer, M. B.; Grabar, K. C.; Jackson, M. A.; Natan, M. J. *J. Phys. Chem.* **1996**, *100*, 718.

(34) Jana, N. R. *Analyst* **2003**, *128*, 954.

(35) Selvakannan, P. R.; Swami, A.; Srisathiyanarayanan, D.; Shirude, P. S.; Pasricha, R.; Mandale, A. B.; Sastry, M. *Langmuir* **2004**, *20*, 7825.

(36) Ji, X. H.; Xu, S. P.; Wang, L. Y.; Liu, M.; Pan, K.; Yuan, H.; Ma, L.; Xu, W. Q.; Li, J. H.; Bai, Y. B.; Li, T. J. *Colloids Surf., A* **2005**, *257*−*258*, 171.

(37) Cao, Y. W. C.; Jin, R. C.; Mirkin, C. A. *Science* **2002**, *297*, 1536.

(38) Cao, Y. C.; Jin, R. C.; Nam, J. M.; Thaxton, S.; Mirkin, C. A. *J. Am. Chem. Soc.* **2003**, *125*, 14676.

(39) Bright, R. M.; Walter, D. G.; Musick, M. D.; Jackson, M. A.; Allison, K. J.; Natan, M. J. *Langmuir* **1996**, *12*, 810.

(40) Rivas, L.; Sanchez-Cortes, S.; Garcia-Ramos, J. V.; Morcillo, G. *Langmuir* **2000**, *16*, 9722.

(41) Srnova-Sloufova, I.; Vlckova, B.; Bastl, Z.; Hasslett, T. L. *Langmuir* **2004**, *20*, 3407.

(42) Lee, P. C.; Meisel, D. *J. Phys. Chem.* **1982**, *86*, 3391.

(43) Srnova-Sloufova, I.; Lednicky, F.; Gemperle, A.; Gemperlova, J. *Langmuir* **2000**, *16*, 9928.

(44) Cai, W. B.; Ren, B.; Li, X. Q.; She, C. X.; Liu, F. M.; Cai, X. W.; Tian, Z. Q. *Surf. Sci.* **1998**, *406*, 9.

(45) Sun, Y.; Mayers, B. T.; Xia, Y. *Nano Lett.* **2002**, *2*, 481.

(46) Sun, Y.; Xia, Y. *Anal. Chem.* **2002**, *74*, 5297.

(47) Sun, Y.; Xia, Y. *J. Am. Chem. Soc.* **2004**, *126*, 3892.

(48) Wyckoff, R. W. G. *Crystal Structures*; Interscience/J. Wiley: New York, 1965; Vol. 1.

(49) Turkevich, J.; Kim, G. *Science* **1970**, 873.

(50) Brown, K. R.; Natan, M. J. *Langmuir* **1998**, *14*, 726.

(51) Osawa, M.; Matsuda, N.; Yoshii, K.; Uchida, I. *J. Phys. Chem.* **1994**, *98*, 12702.

(52) Szafranski, C. A.; Tanner, W.; Laibinis, P. E.; Garrell, R. L. *Langmuir* **1998**, *14*, 3570.

(53) Carron, K. T.; Hurley, L. G. *J. Phys. Chem.* **1991**, *95*, 9979.

(54) Hao, E.; Li, S.; Bailey, R. C.; Zou, S.; Schatz, G. C.; Hupp, J. T. *J. Phys. Chem. B* **2004**, *108*, 1224.